Dynamical study of graphite and graphite intercalation compounds

L. Lang, S. Doyen-Lang, A. Charlier, and M. F. Charlier
Laboratoire de Physique du Solide, Institut de Physique et d'Electronique de Metz, 1 Boulevard François Arago, 57078 Metz Cedex 3, France

(Received 2 June 1993; revised manuscript received 27 September 1993)

We propose a very simple model of lattice dynamics of graphite and its intercalation compounds (GIC's): our model only uses five force constants for graphite, and seven for the GIC. It is used to calculate the dynamical matrix of the structure, and to obtain by matrix diagonalization the phonon vibration frequencies for each element of the first Brillouin zone. Making use of available experimental results concerning graphite as well as LiC_6, we may approximate the parameters introduced in the model. Finally, with the results so obtained, we calculate a great number of physical properties of these compounds: specific heat, Debye temperature θ_D, bidimensional or tridimensional character, as well as elastic constants.

I. INTRODUCTION

Graphite has a layered appearance; this characteristic is due to the great difference between in- and out-of-plane interactions (the important interaction between the atoms in the same plane, as opposed to the very weak interaction between atoms in neighboring planes).[1–3] From this quasibidimensionality comes a large number of properties: important differences between elastic constants parallel and perpendicular to the graphite planes, different conductivities, etc. Graphite and graphite intercalation compounds (GIC's) have been in the past studied from a dynamical point of view, but the proposed models have thus used a great number of adjustable parameters, and the results obtained (phonon dispersion curves as well as state densities) were not used to estimate the physical properties of these materials.

We have attempted here to construct a simple model: only five force constants for graphite and seven for the GIC. This model has allowed us to evaluate a great number of physical properties as often as possible which agree well with available experimental results. It is also important to point out that for graphite and LiC_6, the results obtained add nothing new to what was already known, neither for elastic constants, specific heat, nor the Debye temperature; however, these preliminary calculations allow us to test the model's validity for other compounds.

II. STRUCTURE OF THE COMPOUNDS

A. Graphite structure

Even though graphite may possess two structures, one hexagonal[1,2] and the other rhombohedral, the instability and weak crystallization of the latter is the reason we study only the hexagonal phase of graphite. In hexagonal graphite, the carbon atoms are organized in plane form, called graphitic planes, in which they are placed in the vertices of open hexagons, the edges of which have a length of d_{cc} =1.42 Å (the smallest distance between atoms belonging to the same plane); in addition, graphite possesses a stacking sequence $\mathcal{AB}\cdots$. Indeed, two equivalent atoms in two successive planes are deduced by means of a double translation (see Fig. 1): a translation perpendicular to the graphitic plane ($\vec{c}$ axis) and of length d_{pp}=3.35 Å (the distance between two graphitic planes) and a translation denoted $\vec{\tau}$ of length d_{cc}. The vectors of the primitive cell are

$$\vec{a}_1 = \begin{pmatrix} a \\ 0 \\ 0 \end{pmatrix}, \qquad \vec{a}_2 = \begin{pmatrix} -a/2 \\ a\sqrt{3}/2 \\ 0 \end{pmatrix}, \qquad \vec{a}_3 = \begin{pmatrix} 0 \\ 0 \\ c \end{pmatrix} \tag{2.1}$$

with

$$\begin{aligned} \left\| \vec{a}_1 \right\| = \left\| \vec{a}_2 \right\| &= a = \sqrt{2} d_{cc} = 2.46 \text{ Å}, \\ \left\| \vec{a}_3 \right\| &= c = 2 d_{pp} = 6.70 \text{ Å}. \end{aligned} \tag{2.2}$$

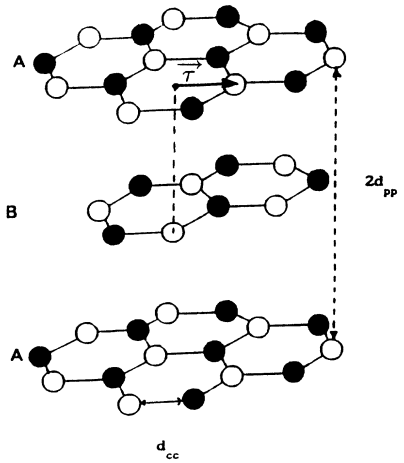

FIG. 1. Structure of hexagonal graphite.

TABLE I. Position of atoms in a graphite structure.

Atom	Position		
	$\vec{a}_1$	$\vec{a}_2$	$\vec{a}_3$
A	0	0	1/4
B	1/3	2/3	1/4
C	0	0	3/4
D	2/3	1/3	3/4

This cell contains four carbon atoms, denoted **A**, **B**, **C**, and **D** (see Table I); these positions correspond to notations $2b$ and $2c$ of the space group $P6_3/mmm$.[4]

B. GIC structure

First-stage GIC studied here are partitioned into two large families, each composed of two subgroups: MC_6 compounds (Li, Ca, Sr, Ba, Sm, Eu, Yb) are present in the form of one- and two-site compounds; MC_8 compounds (K, Rb, Cs) exist in the form of three- and four-site compounds. Furthermore, we study here the LiC_2 compound, recently synthesized, which will allow us to evaluate the influence of a strong intercalate concentration, on the bidimensionality of lithium-based compounds.

All the compounds mentioned above have a hexagonal structure of which the basis vectors are identical to those of graphite. The structure as well as the different cell parameters are listed in Table II.[3–11] Among all of the first-stage GIC, studied here, the stacking sequence is no longer $\mathcal{AB}$, but becomes $\mathcal{AA}$, which means that two successive planes are perfectly superimposed.

III. DYNAMICAL STUDY OF COMPOUNDS

A. The De Launay model

To calculate the dynamical matrix of graphite and GIC, we use the De Launay model.[12] This model assumes that there exists between each atom central forces which depend only on the variation of the distance between two atoms; angular forces which depend only on the angle between the line joining two atoms at any given instant, and the line between the two in equilibrium. The crystal lattice, made up of N atoms in the primitive cell is considered as the sum of N sublattices. Each sublattice contains only one atom, and possesses the symmetry of the crystal. To calculate the equations of motion of the crystal, we take into account the interactions between atoms in the same sublattice, but also those between different sublattices. Furthermore, all the atoms of the same sublattice shall be assumed to vibrate at the same frequency.

1. Central forces

The variation of the distance separating two atoms in a crystal is written as

$$\vec{u}^{\,c}_{0n'ss'} = \left[\vec{\epsilon}_{0n'ss'} \cdot \left(\vec{u}_{0s} - \vec{u}_{n's'}\right)\right] \vec{\epsilon}_{0n'ss'}. \quad (3.1)$$

$\vec{\epsilon}_{0n'ss'}$ is the unit vector defining the direction of the equilibrium position between atoms referenced by the subscripts 0 and n'. The vectors $\vec{u}_{0s}$ and $\vec{u}_{n's'}$ are displacement vectors of the atoms 0 and n', respectively. The force created by such a displacement is of the form

$$\vec{F}^{\,c}_{0n'ss'} = -\alpha \vec{u}^{\,c}_{0n'ss'} \quad (3.2a)$$

$$= -\alpha \left[\vec{\epsilon}_{0n'ss'} \cdot \left(\vec{u}_{0s} - \vec{u}_{n's'}\right)\right] \vec{\epsilon}_{0n'ss'}. \quad (3.2b)$$

This result is the microscopic expression of Hooke's law (the force brought about by a displacement is proportional thereto).

2. Angular forces

In the case of an angular displacement, the expression for $\vec{u}^{\,a}_{0n'ss'}$ is

TABLE II. Cell parameters of graphite and GIC.

Compound	Structure	d_{cc} (Å)	d_{pp} (Å)	a	c	Symmetry group	Positions	
							Carbon	Intercalate
LiC_6	$\mathcal{A}\alpha\mathcal{A}\alpha$	1.435	3.706	$3d_{cc}$	d_{pp}	$P6/mmm$	$6j$	$1b$
LiC_2	$\mathcal{A}(\alpha\beta\gamma)\mathcal{A}(\alpha\beta\gamma)$[a]	1.435	3.706	$\sqrt{3}d_{cc}$	d_{pp}	$P6/mmm$	$2c$	$1b$
CaC_6	$\mathcal{A}\alpha\mathcal{A}\beta$	1.430	4.60	$2d_{cc}\sqrt{3}$	$2d_{pp}$	$P6/mmc$	$12i$	$2d$
SrC_6	$\mathcal{A}\alpha\mathcal{A}\beta$	1.439	4.94	$2d_{cc}\sqrt{3}$	$2d_{pp}$	$P6/mmc$	$12i$	$2d$
BaC_6	$\mathcal{A}\alpha\mathcal{A}\beta$	1.434	5.25	$2d_{cc}\sqrt{3}$	$2d_{pp}$	$P6/mmc$	$12i$	$2d$
SmC_6	$\mathcal{A}\alpha\mathcal{A}\beta$	1.438	4.872	$2d_{cc}\sqrt{3}$	$2d_{pp}$	$P6/mmc$	$12i$	$2d$
EuC_6	$\mathcal{A}\alpha\mathcal{A}\beta$	1.437	4.58	$2d_{cc}\sqrt{3}$	$2d_{pp}$	$P6/mmc$	$12i$	$2d$
YbC_6	$\mathcal{A}\alpha\mathcal{A}\beta$	1.440	4.573	$2d_{cc}\sqrt{3}$	$2d_{pp}$	$P6/mmc$	$12i$	$2d$
KC_8	$\mathcal{A}\alpha\mathcal{A}\beta\mathcal{A}\gamma$[b]	1.432	5.32	$2\sqrt{3}d_{cc}$	$3d_{pp}$	$P6/mmm$	24	3
RbC_8	$\mathcal{A}\alpha\mathcal{A}\beta\mathcal{A}\gamma$[b]	1.431	5.618	$2\sqrt{3}d_{cc}$	$3d_{pp}$	$P6/mmm$	24	3
CsC_8	$\mathcal{A}\alpha\mathcal{A}\beta\mathcal{A}\gamma$[b]	1.431	5.928	$2\sqrt{3}d_{cc}$	$3d_{pp}$	$P6/mmm$	24	3

[a] This notation signifies that the three sites α, β, and γ of the MC_6 structure are occupied, and not that there are three planes of intercalate.

[b] The compounds KC_8 and RbC_8 are in fact the compounds $\mathcal{A}\alpha\mathcal{A}\beta\mathcal{A}\gamma\mathcal{A}\delta$.

$$\vec{u}^{\,a}_{0n's's'} = \left[\vec{\epsilon}_{0n's's'} \wedge \left(\vec{u}_{0s} - \vec{u}_{n's'}\right)\right] \wedge \vec{\epsilon}_{0n's's'}$$

$$= \vec{u}_{0s} - \vec{u}_{n's'} \tag{3.3a}$$

$$- \left[\vec{\epsilon}_{0n's's'} \cdot \left(\vec{u}_{0s} - \vec{u}_{n's'}\right)\right] \cdot \vec{\epsilon}_{0n's's'} \tag{3.3b}$$

and therefore

$$\vec{F}^{\,a}_{0n's's'} = -\alpha\, \vec{u}^{\,a}_{0n's's'}$$

$$= -\alpha \Big\{ \vec{u}_{0s} - \vec{u}_{n's'}$$

$$- \left[\vec{\epsilon}_{0n's's'} \cdot \left(\vec{u}_{0s} - \vec{u}_{n's'}\right)\right] \cdot \vec{\epsilon}_{0n's's'} \Big\}. \tag{3.4}$$

The total force, also called a noncentral force, is written as

$$\vec{F}_{0sn's'\mu} = -\alpha'_\mu \left(\vec{u}_{0s} - \vec{u}_{n's'}\right)$$

$$- (\alpha_\mu - \alpha'_\mu) \left[\vec{\epsilon}_{0n's's'} \cdot \left(\vec{u}_{0s} - \vec{u}_{n's'}\right)\right.$$

$$\left. \times \vec{\epsilon}_{0n's's'}\right], \tag{3.5}$$

μ representing the neighborhood in question.

The equations of motion in a crystal are therefore written in terms of this force:

$$-m_s \frac{\partial^2 u_{0si}}{\partial t^2} = \sum_{n's'\mu} \left(\vec{F}_{0sn's'\mu}\right)_i, \tag{3.6a}$$

$$-m_s\, \omega^2_{si}\, u_{0si} = \sum_{n's'\mu} \Big\{ -\alpha'_\mu \left(\vec{u}_{0s} - \vec{u}_{n's'}\right) (\alpha_\mu - \alpha'_\mu)$$

$$\times \left[\vec{\epsilon}_{n'} \cdot \left(\vec{u}_{0s} - \vec{u}_{n's'}\right) \vec{\epsilon}_n\right] \Big\}_i. \tag{3.6b}$$

This set of $3N$ coupled differential equations (N being the number of atoms in the primitive cell of the crystal) may be rewritten in the form

$$m_s\, \omega^2_{si}\, u_{0si} + \sum_{n's'\mu} \Big\{ -\alpha'_\mu \left(\vec{u}_{0s} - \vec{u}_{n's'}\right) (\alpha_\mu - \alpha'_\mu)$$

$$\times \left[\vec{\epsilon}_{n'} \cdot \left(\vec{u}_{0s} - \vec{u}_{n's'}\right) \vec{\epsilon}_n\right] \Big\}_i = 0; \tag{3.7}$$

this system admits nontrivial solutions if and only if the determinant

$$\left| D(\vec{k}) - m_s\, \omega^2_s(\vec{k}) I \right| = 0 \tag{3.8}$$

is zero. The resolution of the above eigensystem allows us to obtain phonon vibration frequencies $\omega_s(\vec{k})$ in the crystal, as well as the eigenvectors or vibration vectors $\vec{u}_{ns}(\vec{k})$.

B. Graphite

Hexagonal graphite possesses a primitive cell containing four independent atoms; therefore let us consider four sublattices, leading to a 12×12 dynamical matrix. Having taken into account the strong interaction between the carbon atoms nearest each other in the plane (covalent bond of carbon), we limit ourselves in our study of central interactions to the atoms next nearest in the plane and the nearest atoms in the neighboring plane. As for angular interactions, we shall limit ourselves to the nearest neighboring atoms (see Fig. 2). The force constants used for graphite will thus be the following: α_1 and α'_1 for atoms nearest each other in the plane; α_2 for the next nearest atoms in the plane; α_3 and α'_3 for the nearest atoms in the neighboring plane. We may therefore write, taking into account the symmetry of graphite, the dynamical matrix in the form

$$D(\vec{k}) = \begin{pmatrix} A & C^* & E & 0 \\ C & B & 0 & 0 \\ E & 0 & A & C \\ 0 & 0 & C^* & B \end{pmatrix}. \tag{3.9}$$

To establish this matrix, we used the following properties. The **A** and **C** atoms have the same neighborhood: three first neighbors in the plane (a type **B** atom for the type **A**, and **D** for **C**), six second neighbors in the plane (type **A** for **A** and **C** for **C**), and two first neighbors out-of-plane (type **C** for **A** and **A** for **C**); the **B** and **D** atoms have the same neighborhood: three first neighbors in the plane (a type **A** atom for the type **B**, and **C** for **D**), six second neighbors in the plane (type **B** for **B** and **D** for **D**).

The elements A, B, C, and D of the dynamical matrix

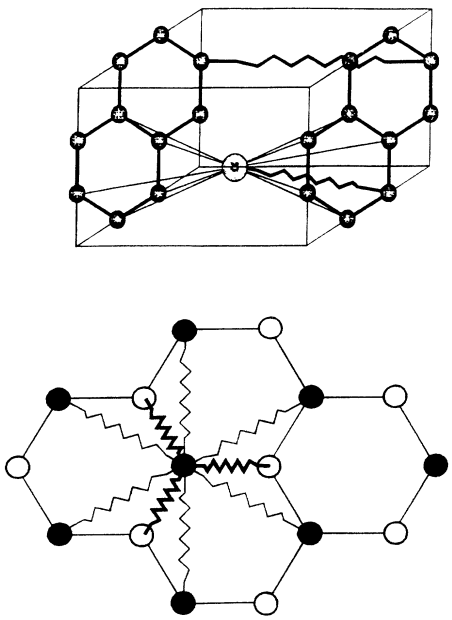

FIG. 2. Atomic force constants of graphite and GIC.

$D(\vec{k})$ are themselves 3×3 matrices: the matrices A and B are expressions of the interaction between the atoms of type **A** and **C** (for matrix A) or **B** and **D** (for matrix B), and themselves take into account the invariance of the dynamical matrix under the action of a rigid-body translation:

$$\sum_i D_{ij}(\vec{k}=\vec{0}) = \sum_i D_{ji}(\vec{k}=\vec{0}) = 0; \qquad (3.10)$$

C is the expression of the interaction between the **A** and **B** or **C** and **D** atoms; E is the expression of the interaction between the **A** and **C** atoms.

C. Graphite intercalation compounds

Given that the strong graphite covalence only adds two force constants to those already chosen for graphite, namely, β_1 and β_1' for interactions between carbon and intercalate atoms. To simplify the notation of dynamical matrices $D(\vec{k})$, we shall write them as a sum of two submatrices, one representing the interactions between carbon atoms $D_{cc}(\vec{k})$, and the other those between carbon and intercalate atoms $D_{ci}(\vec{k})$:

$$D(\vec{k}) = D_{cc}(\vec{k}) + D_{ci}(\vec{k}). \qquad (3.11)$$

Primitive cells of GIC are composed of between 3 (LiC_2) and 27 (MC_8) atoms. This gives us dynamical matrices of rank from 9 to 81.

1. LiC_2

This compound possesses the simplest structure of GIC (only three atoms per cell). This leads us to calculate a dynamical matrix of rank 9:

$$D_{cc}(\vec{k}) = \begin{pmatrix} A & B & 0 \\ B^* & A & 0 \\ 0 & 0 & 0 \end{pmatrix} \qquad (3.12)$$

and

$$D_{ci}(\vec{k}) = \begin{pmatrix} i & 0 & I \\ 0 & i & I^* \\ I^* & I & Li \end{pmatrix}. \qquad (3.13)$$

2. LiC_6

The primitive cell of LiC_6 consists of seven independent atoms, which gives us a 21×21 matrix:

$$D_{cc}(\vec{k}) = \begin{pmatrix} A & B^* & C^* & D^* & C & F^* & 0 \\ B & A & D & C & F & C^* & 0 \\ C & D^* & A & F^* & C^* & B^* & 0 \\ D & C^* & F & A & B & C & 0 \\ C^* & F^* & C & B^* & A & D^* & 0 \\ F & C & B & C^* & D & A & 0 \\ 0 & 0 & 0 & 0 & 0 & 0 & 0 \end{pmatrix} \qquad (3.14)$$

and

$$D_{ci}(\vec{k}) = \begin{pmatrix} i & 0 & 0 & 0 & 0 & 0 & I_1^* \\ 0 & ii & 0 & 0 & 0 & 0 & I_2^* \\ 0 & 0 & iii & 0 & 0 & 0 & I_3^* \\ 0 & 0 & 0 & i & 0 & 0 & I_1 \\ 0 & 0 & 0 & 0 & ii & 0 & I_2 \\ 0 & 0 & 0 & 0 & 0 & iii & I_3 \\ I_1 & I_2 & I_3 & I_1^* & I_2^* & I_3^* & Li \end{pmatrix}. \qquad (3.15)$$

3. MC_6 two sites

Compound of type MC_6 two sites contain 14 atoms per cell, which gives a dynamical matrix of rank 42.

4. MC_8 three sites

Compounds of type MC_8 are normally divided into two families: three-site compounds (RbC_8); four-site compounds (KC_8 and CsC_8). Four-site compounds have a pattern composed of 72 atoms which lead to a Hermitian dynamical matrix of rank 216, yet it has not been possible for us to satisfactorily diagonalize such a system. We shall therefore assume from now on that these compounds possess a structure of the type MC_8 three sites.

IV. RESULTS

A. Force constants

With the use of available experimental results of the Brillouin zone center, labeled Γ (graphite and GIC), and on the zone boundary (graphite), we approximate the force constants α_i and β_i, i.e., the parameters introduced into the dynamical matrix using De Launay's method. For graphite we made the following decision (see Table III): two frequencies in the zone center; three frequencies on the zone boundary: one at A and two at M. To approximate these force constants, we diagonalize the dynamical matrix until we obtain the desired frequencies.

For MC_8 compounds, we had to assume, because of the small number of experimental results, that the force constants bound to the carbon matrix are only slightly different from those of pure graphite. To calculate the force constants, we made use of experimental results obtained by inelastic neutron scattering (Zabel and coworkers[22–27]) as well as those obtained by Raman spectroscopy (Solin and Caswell[18]). The whole of the obtained results for the force constants is listed in Table IV.

TABLE III. Values of frequencies in graphite.

Frequencies	Experimental values	Theoretical models			Calculated values
		Nicholson and Bacon (Ref. 19)	Mani and Ramani (Ref. 20)	Gupta *et al.* (Ref. 21)	
$\nu_{TO}(\Gamma)$	47.64 (Refs. 13 and 14)	47.25	47.28	46.3	47.26
	47.25 (Refs. 13 and 14)	47.25[a]	47.25[a]	46.3	47.24[a]
	1.5 (Ref. 15)	1.26[a]	1.35[a]	1.3	1.35
$\nu_{LO}(\Gamma)$	26.04 (Refs. 16–18)	42.21	19.32	24.2	25.58
		42.21	19.32	24.2	25.58
		42.15	18.90	23.7	25.27
		42.15	18.90	23.7	25.27
	3.81 (Ref. 15)	3.81[a]	3.78[a]	3.9	3.81[a]
				1.3	1.35
$\nu_{TO}(A)$		47.25	47.25[a]	46.1	47.25
$\nu_{LO}(A)$		42.18	41.91	23.7	25.42
$\nu_{LA}(A)$	2.70 (Ref. 15)	2.70	2.70[a]	2.7	2.72[a]
$\nu_{TA}(A)$	0.99 (Ref. 15)	0.90	0.99[a]	0.84	0.97[a]
$\nu_{TA}(M)$	14.19 (Ref. 15)	14.28	14.19[a]	16.1	14.59[a]

[a]Values used to fit the force constants.

B. Phonon dispersion curves—density of states

Using the previously calculated force constants, we graph the phonon dispersion curves of these compounds. These theoretical curves agree with existing experimental data (see Fig. 3 and Table V).

State density is obtained by diagonalizing many times the dynamical matrix for the element points of the first Brillouin zone. It should be pointed out that on the phonon state density curves (see Fig. 4) the graphitic character of the compounds studied here stands out: indeed, we may observe on all of the curves that the density peaks at 22 and 47 THz characteristic of graphite are found on most. But the more the compound is concentrated, the more the interaction between carbon and intercalate atoms takes precedence over those that are bound to the graphitic structure (as in the case of LiC_2).

C. Specific heat and Debye temperature

Using the state density $g(\nu)$, we may evaluate the specific heat of different compounds. Indeed, C_v depends on $g(\nu)$ by the relation

$$C_v = k_B \int_0^{\nu_{\max}} \left(\frac{h\nu}{k_B T}\right)^2 \frac{e^{h\nu/k_B T} g(\nu)}{\left(e^{h\nu/k_B T}-1\right)^2}\, d\nu = k_B \sum_{\nu_i} \left(\frac{h\nu_i}{k_B T}\right)^2 \frac{e^{h\nu_i/k_B T} g(\nu_i)}{\left(e^{h\nu_i/k_B T}-1\right)^2}. \quad (4.1)$$

This last relation allows us to calculate the specific heat of graphite and of different GIC's studied here. The specific heat of graphite thus obtained might have been compared with that of experimental measurements performed by De Sorbo and Tyler,[28] and Spencer,[29] as well as Krumhansl and Brooks;[30] the agreement is good at every point (see Fig. 5), and comparable to that obtained by Young and Koppel.[31]

The development of specific heat in the neighborhood of 0 K has allowed us to distinguish two zones, the first for temperatures less than 6 K and the second for temperatures between 6 and 160 K, inclusive.

1. *Development for $T < 6$ K: Calculation of θ_D*

In the neighborhood of absolute zero, we may approximate the specific heat conforming to Debye's theory in

TABLE IV. Atomic force constants (in $N\,m^{-1}$).

Compound	Carbon-carbon interactions					Carbon-intercalate interactions	
	α_1	α_1'	α_2	α_3	α_3'	β_1	β_1'
Graphite	505.1	84.4	73.7	5.92	0.72		
LiC_6, LiC_2	568.7	21.5	68.2	2.13	0.245	27.95	3.47
CaC_6, BaC_6	486.0	81.4	66.4	3.51	0.295	3.2	0.15
SrC_6, SmC_6	486.0	81.4	66.4	3.51	0.295	3.2	0.15
EuC_6, YbC_6	486.0	81.4	66.4	3.51	0.295	3.2	0.15
CsC_8	491.5	83.6	66.7	3.51	0.242	5.6	0.35
KC_8	491.5	83.6	66.7	3.51	0.242	3.5	0.25
RbC_8	491.5	83.6	66.7	3.51	0.242	4.2	0.28

TABLE V. Values of frequencies in lithium intercalation compounds.

Compound	Experimental values	Gupta *et al.*	Calculated
LiC_6	50.4		50.5
	47.25	46.2	47.5
	45.09		
	34.8		39.1
	32.4		
	24.3	25.2	22.5
	19.5		20.8
	13.5	12.9	13.6
	12.45		12.0
LiC_2	49.8		
	47.4		47.4
	35.1		
	30.9		
	26.4		
	24.3		
	19.8		
	13.8		14.0
	12.8		10.0

the form of a T^3 law:

$$C_v = \gamma T^3 + \alpha T, \tag{4.2}$$

the γ being related to the Debye temperature by the relation

$$\theta_D = \left(\frac{12\pi^4 N k_B}{5\gamma}\right)^{1/3}. \tag{4.3}$$

Results thus calculated are presented in Table VI.

2. *Development for $T \in [6, 160]$ K: Graphite and GIC anisotropy*

Graphite is characterized by an abnormal specific heat: indeed, we observe a variation of the specific heat C_v in the form of a "T^2" law, instead of the classical "T^3" law that holds for three-dimensional crystals. This behavior is due to the great anisotropy of graphite: the interactions between atoms belonging to the same plane (covalent bonds) are extremely strong compared to those existing between planes (π-type orbital bonds). This behavior may be observed in the force constants: α_1, the force constant corresponding to in-plane first-neighbor interactions, is about 100 times more important than α_3, which corresponds to out-of-plane first-neighbor interactions. To show the dependence on "T^2" of the specific heat, we approximate C_v (for temperatures between 6 and 160 K, inclusive) by an exponential law of the type

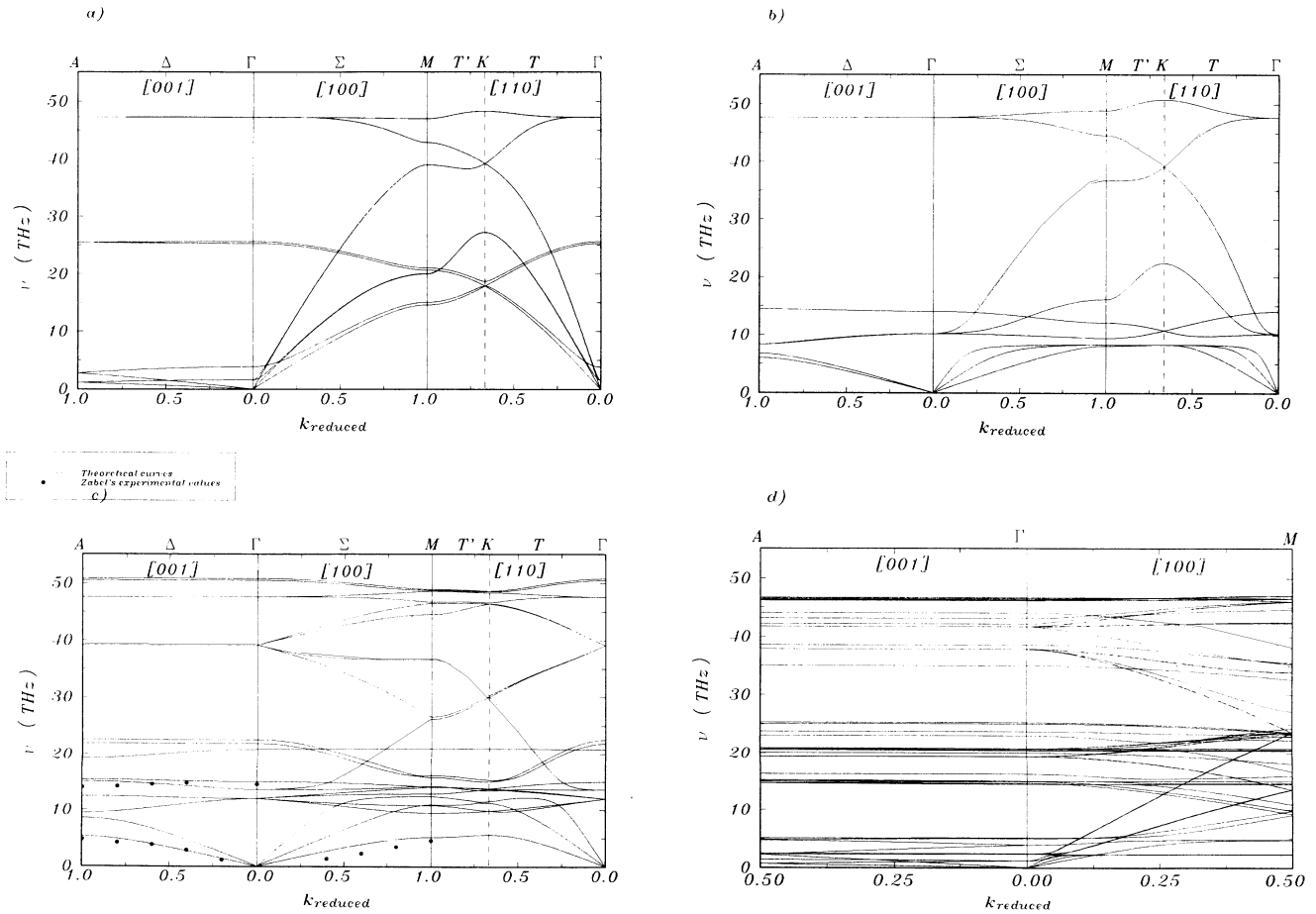

FIG. 3. Phonon dispersion curves of (a) graphite, (b) LiC_2, (c) LiC_6 (dots represent Zabel's experimental values), (d) KC_8.

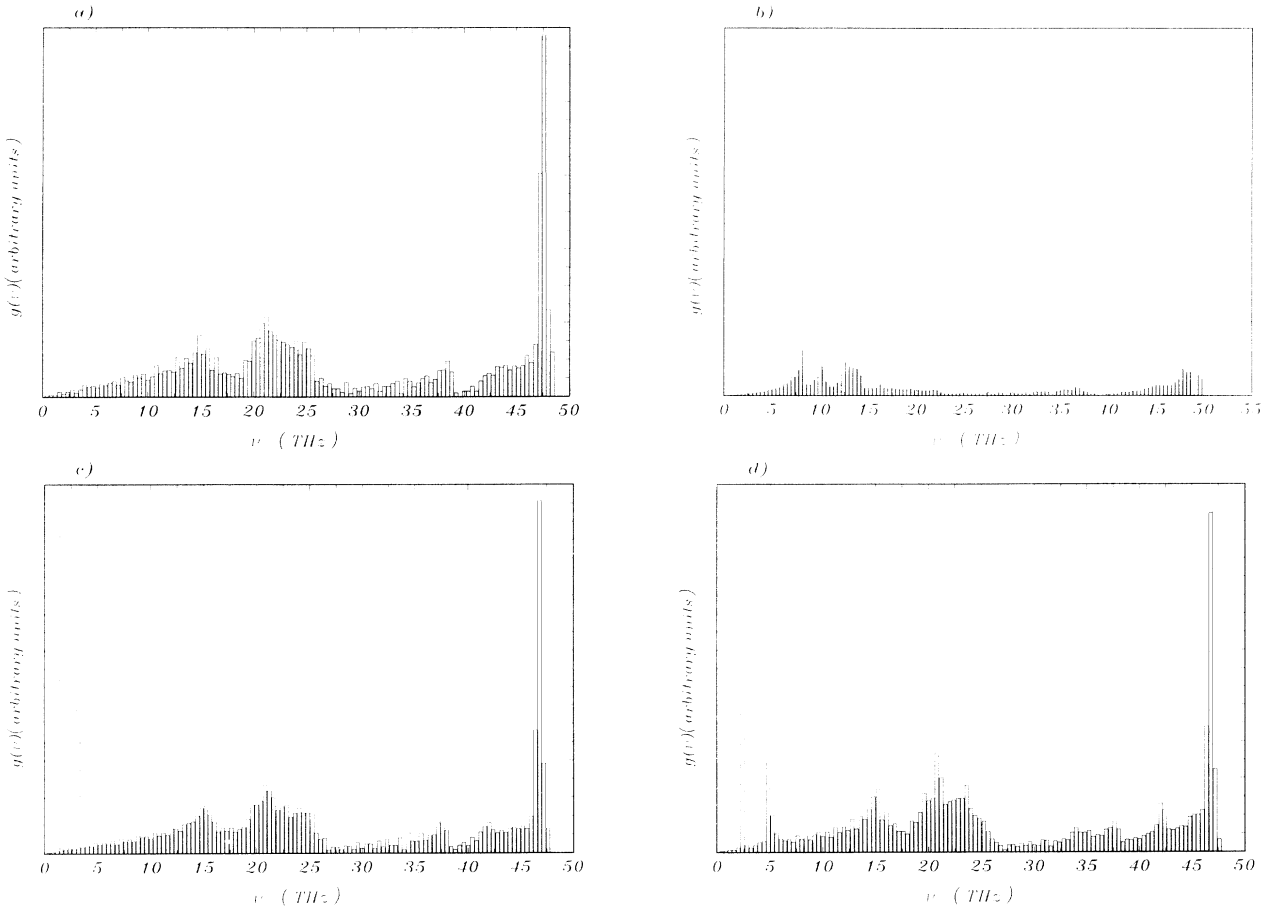

FIG. 4. Phonon density of states of (a) graphite, (b) LiC_2, (c) BaC_6, (d) KC_8.

$$C_v = \beta T^n. \tag{4.4}$$

The best approximation (for χ^2 criterion) allows us to obtain the parameters introduced in this expression (see Table VII). This table reveals the following facts.

In agreement with experimental results, graphite possesses a marked bidimensional character ($n = 2.01 \simeq 2$).

TABLE VI. Values of θ_D for graphite and intercalation compounds.

Compound	Calculated values		Experimental θ_D
	γ (J mol^{-1} K^{-4})	θ_D (K)	
Graphite	2.521×10^{-5}	423.6	413 (Ref. 32), 421 (Ref. 33)
LiC_6	8.85×10^{-6}	603	590 (Refs. 34 and 35)
LiC_2	6.93×10^{-6}	652	
CaC_6	9.70×10^{-6}	585	
BaC_6	1.08×10^{-5}	565	
SrC_6	2.10×10^{-5}	452	
SmC_6	1.77×10^{-5}	479	
EuC_6	1.85×10^{-5}	472	
YbC_6	1.84×10^{-5}	472	
KC_8	7.79×10^{-5}	292	235 (Ref. 33)
RbC_8	6.23×10^{-5}	314	
CsC_8	10^{-5}	321	341 (Ref. 33)

For MC_6 two-site compounds, we observe that the larger the mass of the intercalate, the more the compound is bidimensional (see Fig. 6). We may explain this by the fact that when the mass of the atom increases (up to 173 for ytterbium), the inertia of the intercalate planes also increase, and therefore the vibrations of the

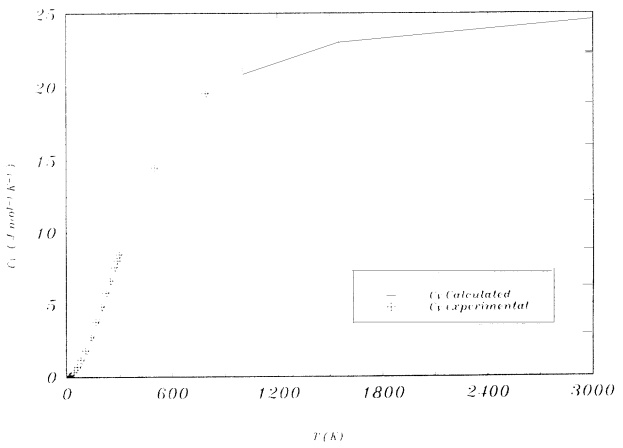

FIG. 5. Comparison of graphite experimental and theoretical specific heat C_v.

TABLE VII. Anisotropy of graphite and its intercalation compounds.

Compound	Exponent
Graphite	2.01
LiC_6	2.83
LiC_2	2.97
CaC_6	2.82
SrC_6	2.26
BaC_6	2.06
SmC_6	2.03
EuC_6	2.02
YbC_6	2.03
KC_8	2.98
RbC_8	2.52
CsC_8	2.49

graphitic plane may not be transmitted. This gives us a system of graphitic planes that vibrate independently of one another, and therefore the system is quasibidimensional.

For MC_8 three-site compounds, we may observe in a lesser fashion the same properties as previously shown.

D. Elastic constants

Another property related to the phonon dispersion curves is the knowledge of the elastic constants of a material. Indeed, this depends on the velocity of the sound in the crystal; now, this velocity is a function of the slope of the dispersion curves for the acoustical branches [those for which $\omega(\vec{k} = \vec{0}) = 0$].

For hexagonal crystals, the elastic constant tensor $[C_{ij}]$ contains only five constants instead of 21 in the general case:

$$[C_{ij}] = \begin{bmatrix} C_{11} & C_{12} & C_{13} & 0 & 0 & 0 \\ C_{12} & C_{11} & C_{13} & 0 & 0 & 0 \\ C_{13} & C_{13} & C_{33} & 0 & 0 & 0 \\ 0 & 0 & 0 & C_{44} & 0 & 0 \\ 0 & 0 & 0 & 0 & C_{44} & 0 \\ 0 & 0 & 0 & 0 & 0 & C_{66} \end{bmatrix} \tag{4.5}$$

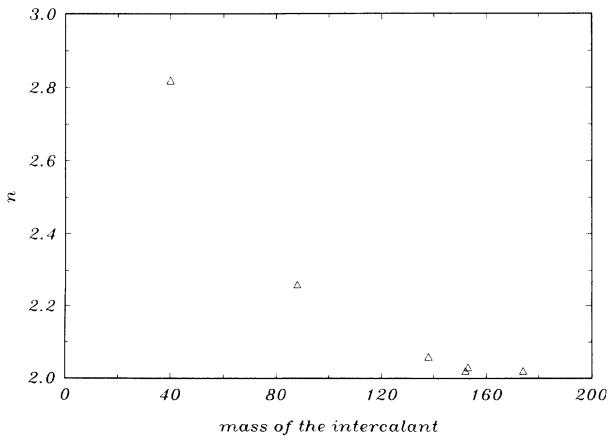

FIG. 6. Evolution of the bidimensionality for MC_6 GIC. Mass in amu.

with $C_{66} = \frac{1}{2}(C_{11} - C_{12})$. The equations of motion for an elastic crystal are of the form

$$\rho \frac{\partial^2 u}{\partial t^2} = \frac{\partial \sigma_{xx}}{\partial x} + \frac{\partial \sigma_{xy}}{\partial y} + \frac{\partial \sigma_{xz}}{\partial z}. \tag{4.6}$$

The constants σ_{ij} are the components of the constraint vector, and u is the x component of the displacement vector. Two similar differential equations exists along the y and z axes, also. The elastic constant tensor may be introduced by using the relation between stress and strain:

$$\sigma_i = \sum_{j=1}^{6} C_{ij}\epsilon_j. \tag{4.7}$$

The subscripts i and j represent the six unequal combinations of the three axes (see Table VIII).

The combination of these two equations leads us to the following determinant:

$$\begin{vmatrix} a_{11} & a_{12} & a_{13} \\ a_{12} & a_{22} & a_{23} \\ a_{13} & a_{23} & a_{33} \end{vmatrix} = 0, \tag{4.8a}$$

with

$$\begin{aligned} a_{11} &= C_{11}k_1^2 + C_{66}k_2^2 + C_{44}k_3^2 - \rho\omega^2, \\ a_{12} &= (C_{12} + C_{66})\,k_1k_2, \\ a_{13} &= (C_{13} + C_{44})\,k_1k_3, \\ a_{22} &= C_{66}k_1^2 + C_{11}k_2^2 + C_{44}k_3^2 - \rho\omega^2, \\ a_{23} &= (C_{13} + C_{44})\,k_2k_3, \\ a_{33} &= C_{44}k_1^2 + C_{44}k_2^2 + C_{33}k_3^2 - \rho\omega^2. \end{aligned} \tag{4.8b}$$

For the direction [100] ($k_1 = k, k_2 = k_3 = 0$) this determinant becomes

$$\begin{vmatrix} C_{11}k^2 - \rho\omega^2 & 0 & 0 \\ 0 & C_{66}k^2 - \rho\omega^2 & 0 \\ 0 & 0 & C_{44}k^2 - \rho\omega^2 \end{vmatrix} = 0. \tag{4.9}$$

If, in addition, we consider the case of a longitudinal wave, we obtain

$$C_{11} = \rho \frac{\omega^2_{\mathrm{LA}[100]}}{k_1^2} \tag{4.10}$$

for a transversal wave along the y axis:

$$C_{66} = \rho \frac{\omega^2_{\mathrm{TA}_1[100]}}{k_1^2}. \tag{4.11}$$

For waves propagating along the direction [001] we obtain

TABLE VIII. Indexing of the elastic tensors.

Index	Direction
1	xx
2	yy
3	zz
4	yz or zy
5	xz or zx
6	xy or yx

TABLE IX. Elastic constants (in 10^{10} N m^2).

Compound	Our calculated values				Experimental values			
	C_{11}	C_{33}	C_{44}	C_{66}	C_{11}	C_{33}	C_{44}	C_{66}
graphite (Refs. 36 and 37)	113	3.74	0.44	38.8	106	3.65	0.40	44
LiC_6	74.7	4.71	1.5	39.1			1.0	
LiC_2	87.71	10.67	8.33	20.57				
BaC_6	101	9.9	0.85	35				
CaC_6	134	15.0	1.05	46				
SrC_6	166	21.0	1.17	57				
SmC_6	202	19.4	1.36	69				
EuC_6	191	20.8	1.45	66				
YbC_6	223	20.0	1.49	77				
KC_8	109	3.57	0.314	38.3		4.85	0.282	
RbC_8	138	5.07	0.384	48.4		4.84		
CsC_8	165	6.07	0.405	58.2		5.83	0.405	

$$C_{33} = \rho\frac{\omega^2_{\mathrm{LA}[001]}}{k_3^2}, \quad C_{44} = \rho\frac{\omega^2_{\mathrm{TA}[001]}}{k_3^2}. \tag{4.12}$$

$\omega_{\mathrm{TA}[001]}$ is twice degenerated, which conforms to that which we may observe on the phonon dispersion curves of graphite and GIC. Using the previous expressions for elastic constants as well as for the slopes of the acoustic branches, we may calculate C_{ij} (see Table IX). This table shows a close agreement between the elastic constants which are calculated and obtained experimentally for graphite[36,37] and GIC.[22–27]

V. CONCLUSIONS

As long as we consider only graphite, this work produces nothing new, but it has allowed us to test the validity of the model used for GIC. Having presented the particularity of being layered, graphite has known a great interest during the past fifty years. Even though the model chosen here is quite simple (only five force constants for graphite, and seven for GIC), the results obtained for thermodynamic properties (C_v and θ_D) as well as for elastic properties are in good agreement with both experimental and theoretical results. In comparison with one of the most accurate models, previously propounded by Maeda, Kuramoto, and Horie, which introduced 8 force constants in the case of graphite[38] and 10 for the GIC.[39] We also obtain a satisfactory agreement for the frequency of the A_{2u} mode (at 26 THz) of graphite shown by the experiment of Solin, Nemanich, and Lucowsky.[16] We have solved the problem resulting from the lack of knowledge of the interaction between the intercalate atoms, interactions which these former authors were not able to evaluate because of the few experimental results available. In their model these interactions were supposed to be the same as those of the potassium metal.

Concerning results obtained for LiC_2, we could only compare them with those proposed by Nalimova *et al.*[40] for the vibration frequencies in the Brillouin zone center Γ. These are in agreement for a great number of frequencies. There remains, however, a problem; indeed, this publication shows nine frequency measurements in Γ, but the primitive cell of LiC_2 contains only three inequivalent atoms, which leads to nine phonon dispersion branches of which three are acoustic (ν=0). We may assume two causes for these three supplementary frequencies. The assumed structure of LiC_2 is not correct; there could coexist two intercalate planes between two successive graphitic planes. The compound which possesses a strong instability[41] could be partially decomposed, and there could exist several kinds of lithium GIC (LiC_6, LiC_3,...). The latter explanation may also explain the strong similarity between measured frequencies for LiC_2 and LiC_6.

For MC_6 two-sites compounds, there exist today only a few experimental and theoretical results; we have thus tried to calculate a great number of constants for these bodies, to have a first approximation of the properties of the compounds, especially of their bidimensional behavior. It should be pointed out, however, that the knowledge of thermodynamic properties (of specific heat, for example) may not be complete without the introduction of anharmonic components into the dynamical matrix. Indeed, the harmonic model is not entirely sufficient to model carbon-intercalate interactions.

Even if the model is not completely satisfactory for thermodynamical properties of compounds, the properties at 0 K (elastic constants and phonon dispersion curves) are not affected by this approximation. We were finally able to show that the bidimensionality of GIC depends mostly on the mass of the intercalate atoms. This behavior is explained by the fact that the intercalate planes become too heavy, and therefore their inertia decouples the vibrations between the neighboring graphitic planes and thus allow us to obtain a system of planes independent one from the other.

ACKNOWLEDGMENT

We are indebted to J.H. Covington for translating this paper from French to English.

[1] J.D. Bernal, Proc. R. Soc. London **106**, 749 (1924).
[2] C. Mauguin, Bull. Soc. Fr. Min. **49**, 32 (1926).
[3] *Collection de Chimie Physique* (Masson & Cie, Paris, 1965).
[4] T. Hahn, *Table for Cristallography* (Kluwer Academic, Dordrecht, 1989), Vol. A.
[5] D. Guerard and A. Herold, Carbon **13**, 337 (1975).
[6] D. Guerard, C. Zeller, and A. Herold, C. R. Acad. Sci. (Paris) **283**, 437 (1976).
[7] A. Herold, Intercalated Mat. **6**, 323 (1979).
[8] P. Lagrange, D. Guerard, and A. Herold, Ann. Chim. **3**, 143 (1978).
[9] D. Guerard, P. Lagrange, M. El Makrini, and A. Herold, Carbon **16**, 285 (1978).
[10] M. El Makrini, D. Guerard, P. Lagrange, and A. Herold, Physica **99B**, 480 (1980).
[11] A. Charlier, M.F. Charlier, and D. Fristot, J. Chem. Phys. Sol. **50**, 987 (1989).
[12] J. De Launay, Solid State Phys. **3**, 203 (1957).
[13] L.J. Brillson, E. Burstein, A.A. Maradudin, and T. Stark, in *Physics of the Semimetals and Narrow Gap Semiconductors, Texas, 1960*, edited by D.L. Carter and R.T. Rate (Pergamon, New York, 1960), p. 187.
[14] F. Tuinstra and J.L. Koenig, J. Chem. Phys. **53**, 1126 (1970).
[15] R. Nicklow, N. Wakabayashi, and H.G. Smith, Phys. Rev. B **5**, 4951 (1972).
[16] S.A. Solin, R.J. Nemanich, and G. Lucowsky, Mater. Sci. Eng. **31**, 159 (1977).
[17] S.A. Solin, P. Chow, and H. Zabel, Phys. Rev. Lett. **53**, 1927 (1984).
[18] S.A. Solin and N. Caswell, J. Raman Spectrosc. **10**, 129 (1981).
[19] A.P.P. Nicholson and D.J. Bacon, J. Phys. C **10**, 2295 (1977).
[20] K.K. Mani and R. Ramani, Phys. Status Solidi B **61**, 659 (1974).
[21] H.C. Gupta, J. Malhotra, N. Rani, and B.B. Tripathi, Mater. Sci. Eng. **85**, 187 (1987).
[22] H. Zabel, A. Magerl, and J.J. Rush, Phys. Rev. B **27**, 3930 (1983).
[23] A. Magerl, H. Zabel, and J.J. Rush, Synth. Met. **7**, 339 (1983).
[24] H. Zabel and A. Magerl, Phys. Rev. B **25**, 2463 (1982).
[25] A. Magerl and H. Zabel, Solid State Sci. **38**, 180 (1981).
[26] H. Zabel, W.A. Kamitakahara, and R. Nicklow, Phys. Rev. B **26**, 5919 (1982).
[27] W.A. Kamitakahara, H. Zabel, and R. Nicklow, in *Intercalated Graphite*, edited by M.S. Dresselhaus *et al.*, MRS Symposia Proceedings No. 20 (Materials Research Society, Pittsburgh, 1983), p. 311.
[28] W. De Sorbo and W.W. Tyler, J. Chem. Phys. **21**, 1660 (1953).
[29] H.M. Spencer, J. Ind. Eng. Chem. **40**, 2152 (1948).
[30] J. Krumhansl and H. Brooks, J. Chem. Phys. **21**, 1663 (1953).
[31] J.A. Young and J.U. Koppel, J. Chem. Phys. **42**, 357 (1965).
[32] M. Van der Hoeven and P. Keesom, Phys. Rev. **130**, 1318 (1963).
[33] U. Mizutani, N. Suganuma, and T. Kondow, Solid State Sci. **38**, 282 (1981).
[34] P. Delhaes, J.C. Rouilleau, J.P. Manceau, D. Guerard, and A. Herold, J. Phys. (Paris) Lett. **37**, L-127 (1976).
[35] P. Delhaes, Mater. Sci. Eng. **31**, 225 (1977).
[36] O.L. Blacksee, D.G. Proctor, E.J. Seldin, G.B. Spence, and T. Weng, J. Appl. Phys. **41**, 3373 (1970).
[37] E.J. Seldin and C.W. Nezbeda, J. Appl. Phys. **41**, 3389 (1970).
[38] M. Maeda, Y. Kuramoto, and C. Horie, J. Phys. Soc. Jpn. **47**, 337 (1979).
[39] C. Horie, M. Maeda, and Y. Kuramoto, Physica **99B**, 430 (1980).
[40] V.A. Nalimova, G.N. Bondarenko, V.L. Kofman, V.V. Adveev, and K.N. Semenenko, in *Proceedings of the 20th Biennial Conference on Carbon, Santa Barbara, 1990* (American Carbon Society, Santa Barbara, 1990), p. 684.
[41] I.T. Belash, A.D. Bronnikov, O.V. Zharikov, and A.V. Palninchenko, Synth. Met. **36**, 283 (1990).

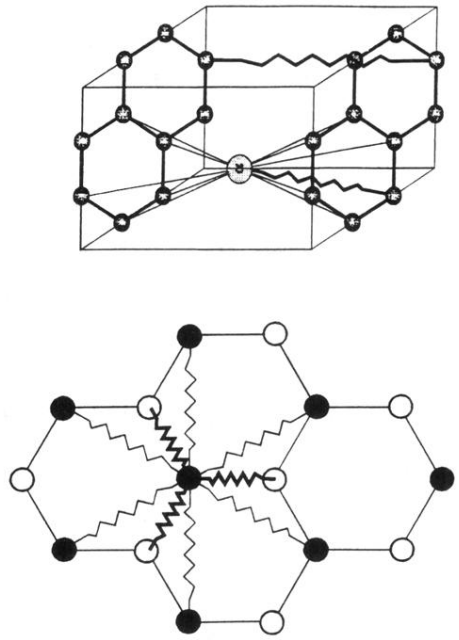

FIG. 2. Atomic force constants of graphite and GIC.